Paper 38

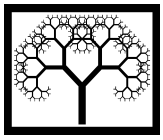

Proceedings of the Eighth International Conference
on Engineering Computational Technology,
B.H.V. Topping, (Editor),
Civil-Comp Press, Stirlingshire, Scotland

Using a Model of Hysteresis for Linearization of Piezo Bender Distortion

M. Pelic and R. Staniek
Institute of Mechanical Technology
Poznan University of Technology, Poland

Abstract

A piezoelectric element can be implemented as a micro drive in many precise applications. In one of them, a piezoelectric element is used as an electro-mechanical actuator in the form of a beam with the element attached to one side. The change of supplied voltage causes a change to the position its free end. When the piezobender actuator is controlled by voltage, the displacement of its free end depends on the difference in electric potentials supplied to its plates and on the actuator's previous states. In the drive application an important parameter is the linearity of the characteristic of the actuators position. A distortion having the biggest impact on these characteristics is hysteresis.
In this paper the model of open loop linearizing controller built on basis of piezobender hysteresis was presented. The principle operation of the controller is based on following the outer contour of the hysteresis loop which is scaled and rotated on a plane supplied voltage as an input signal and the position of the piezobender free end as response. The method of data acquisition and preparation for a hysteresis linearizing, algorithm for generating a correcting signal was shown. Also the results of the simulation were shown and discussed.

Keywords: piezo bender, hysteresis, linearization, neural network.

1 Introduction

A piezo bender actuator is a flat beam-shaped, unilaterally mounted electromechanical drive [1,2]. Consequently, the delineation of its free beam-end is ambiguous, and depends on the driving voltage as well as the retroactive status [3, 4, 5, 6]. Positioning tasks demand linearity of the drive transitory state. However, significant non-linearity is an inherent feature of the piezo bender actuator control voltage, and is predominantly influenced by its hysteresis.

Piezoelectric bending actuator is characterized by two active (work) surfaces that change their geometric properties due to applied voltage, and idle surfaces, whose

geometric distortions are negligible as compared to those of work surfaces. Blocking forces generated by piezoelectric actuators range from 0.5 to 5.5 N, while their normal displacement reaches ± 80 - 1400 µm, and resonant frequencies span from 0.1 to 2.0 kHz. Figure 1 depicts the structure of a typical piezo bender actuator, and includes a description of its surfaces as well as its mounting diagram, while work parameters of two selected actuators are exemplified in Table 1 [7, 8].

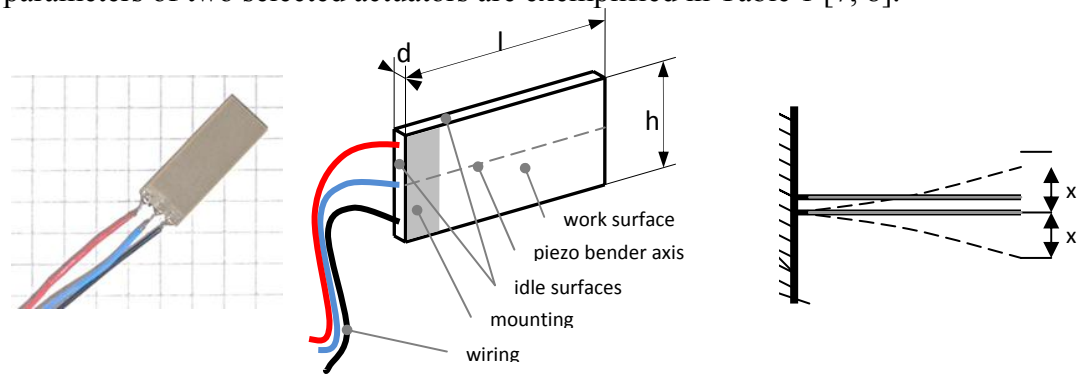

Figure 1: Structure of a typical piezo bender actuator; surface and mounting.

	Noliac	PI Ceramic
Type	CMBP 03	PL112.10
Dimension l, h, d	21mm, 7.8mm, 1.8mm	17,8mm 9.6mm, 0.65mm
Nominal displacement	±85µm	±80µm
Blocking force	5.5N	2N
Resonant frequency	1880Hz	1000Hz
Operating voltage	±100V	±30V
Capacitance	2x435nF	2x1100nF

Table 1: Selected parameters of two piezoelectric actuators.

The described drives were implemented in control stages of Rexroth 4WSE2E electrohydraulic servo valves, substituting torque motors [9]. Figures 2 and 3 show the servo valve structure, the diagram of a flapper plate in control stage, and the device equipped with the piezo actuator.

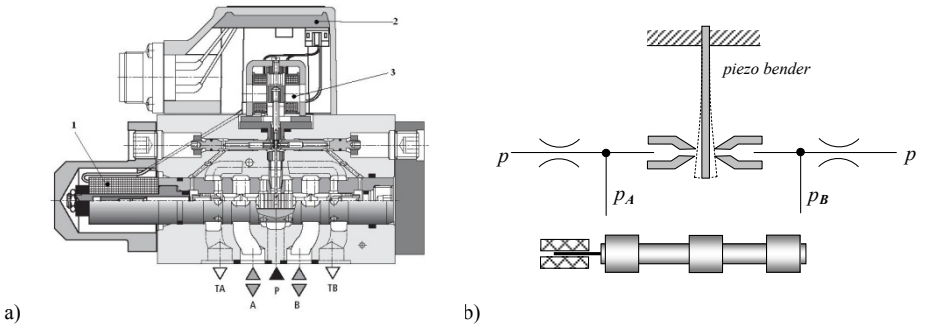

Figure 2: Piezo actuator implementation in Rexroth electrohydraulic servo valve, a) servo valve structure: 1 – slide position sensor, 2 – electronic control system, 3 –torque motor, b) piezo bender as servo valve flapper plate for electric feedback.

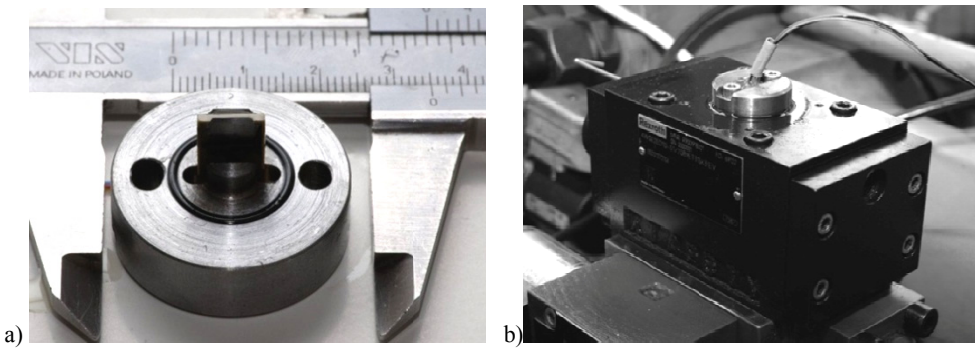

Figure 3: Piezo bender installed in the servo valve,
a) valve head equipped with piezoelectric bender actuator, b) view of servo valve.

The character of the piezo actuator performance applied to the control stage (frequency limit reaching 200 Hz) allowed focusing on quasi-static non-linearity compensation and justified overlooking the dynamic aspects. Under the described experimental circumstances, the piezo bender constraint is approximately static and symmetric, causing a symmetrical hysteresis flattening [10, 11], as opposed to an unencumbered drive working in air.

2 Investigation of piezo bender actuator hysteresis

A work station comprising two general-purpose computers (PCs) was utilized to investigate the quasi-static characteristics of the piezo bender actuator. The first PC, equipped with an input-output RT-DAC4 card constituting a digital-analog interface, was employed as a signal generator based on the real time software, Matlab/Simulink RT WorkShop. The analog signal was directed to the power amplifier (power voltage: ± 32 V, amplification: k = 5) and subsequently to the lining of the piezo bender actuator (Figure 4); the actuator free end displacement was measured by the contactless sensor, Philtec D21 (Figure 5). The second PC was set up with the measurement path acquisition software, Catman, and the MGCplus amplifier. Figure 6 depicts a block diagram of the utilized work station.

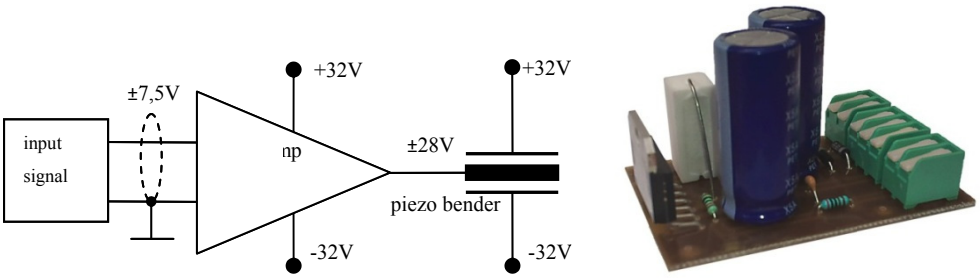

Figure 4: Integration of the piezo bender actuator into the end-amplifier & the view of the amplifier employed in the investigation.

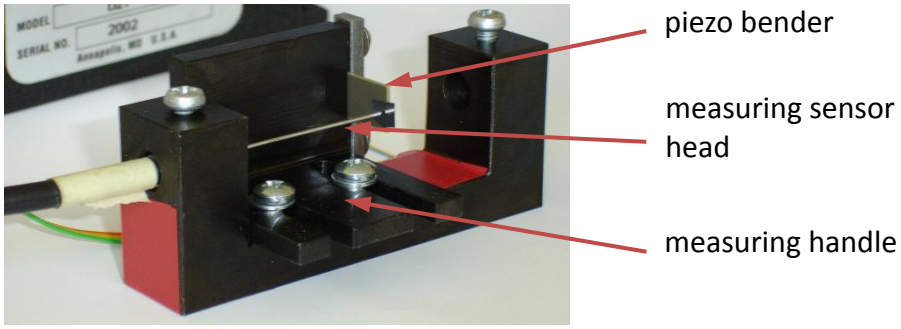

Figure 5: Measuring handle with the investigated piezo bender and the measuring sensor head.

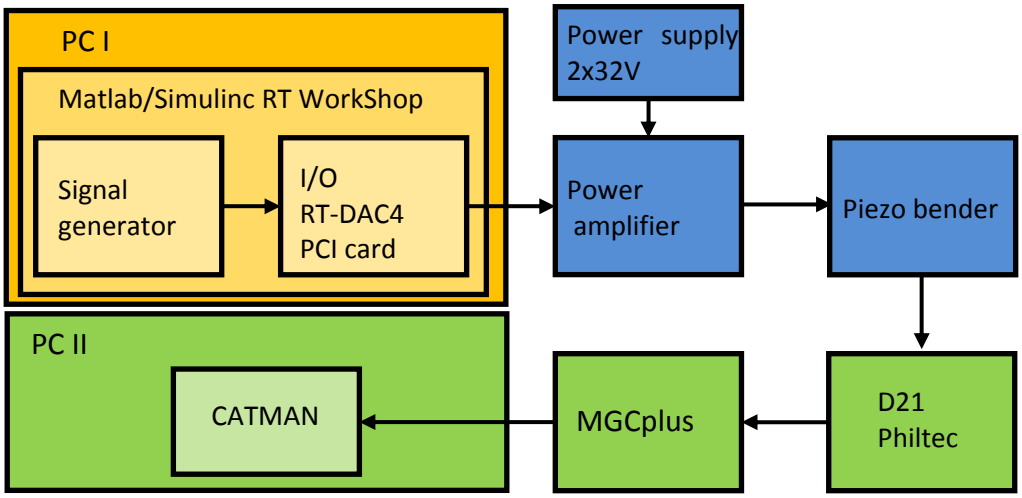

Figure 6: Block diagram of the piezo bender actuator investigation work station.

Figure 7 illustrates the hysteresis family of Pi Ceramic piezo bender actuator. The presented traits were delineated for sinusoidal constraints characterized by a frequency of 0.5 Hz and amplitude of 1 – 7 V. A saturation area can be discerned beyond the control voltage (CV) value of 5.5 V. The phenomenon arises from the power amplifier saturation (CV of 5.5 V * 5 system amplification = 27.5 V) at the power voltage of ± 32 V.

3 Hysteresis compensation

The most commonly used systems for piezo actuator static non-linearity compensation comprise: closed feedback loop systems, feed-forward regulators [12-18], charge amplifiers [19], and compensating setups based on reverse drive profiles.

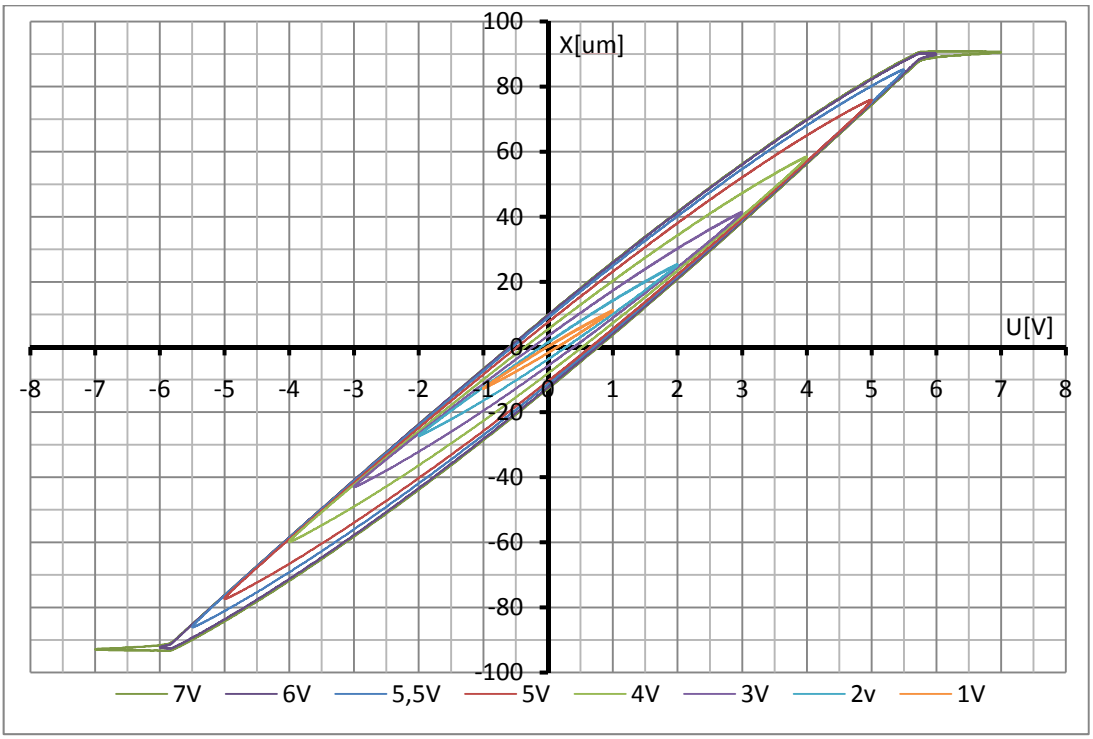

Figure 7: Investigation outcome for piezo bender actuator Pi Ceramic with 1 – 7 V constraint range.

The latter consist in hysteresis generation by means of widely utilized hysteresis models obtained by, among others, the Presiach method [20, 21, 22], leastsquares[23, 24], Bouc-Wen[25], neural networks[26-31] and others[32-41]. The hereby proposed, innovative compensating system applies reverse profiling of the investigated drive developed through outer hysteresis loop transformation. The processing of the modeling data, collected during experimental drive testing, resulted in determination of the quasi-static profile family, constituting a defined set of drive responses to the periodic constraints of various amplitudes. Subsequently, a hysteretic loop of the piezo bender controlled by a periodic U signal of maximal allowed amplitude (no system saturation) was selected, followed by point minimum, $P_1(U_1,X_1)$ and point maximum, $P_2(U_2, X_2)$ constraining signal value determination. The loop was then divided into two arms, corresponding to the increasing and decreasing driving signal, U. Thus adapted data set allowed calculating the value of adjustment signal U_A, constituting the difference between the signal U_n – a constraint resulting in displacement X_n – and U'_n, being the constraint of a linear function of X_n, crossing points P_1 and P_2. Figure 8 depicts the outer hysteretic loop divided into two arms of increasing (f_{H1}) and decreasing (f_{H2}) constraint, with marked points: P_1 & P_2, and values: U_n, U'_n, & X_n.

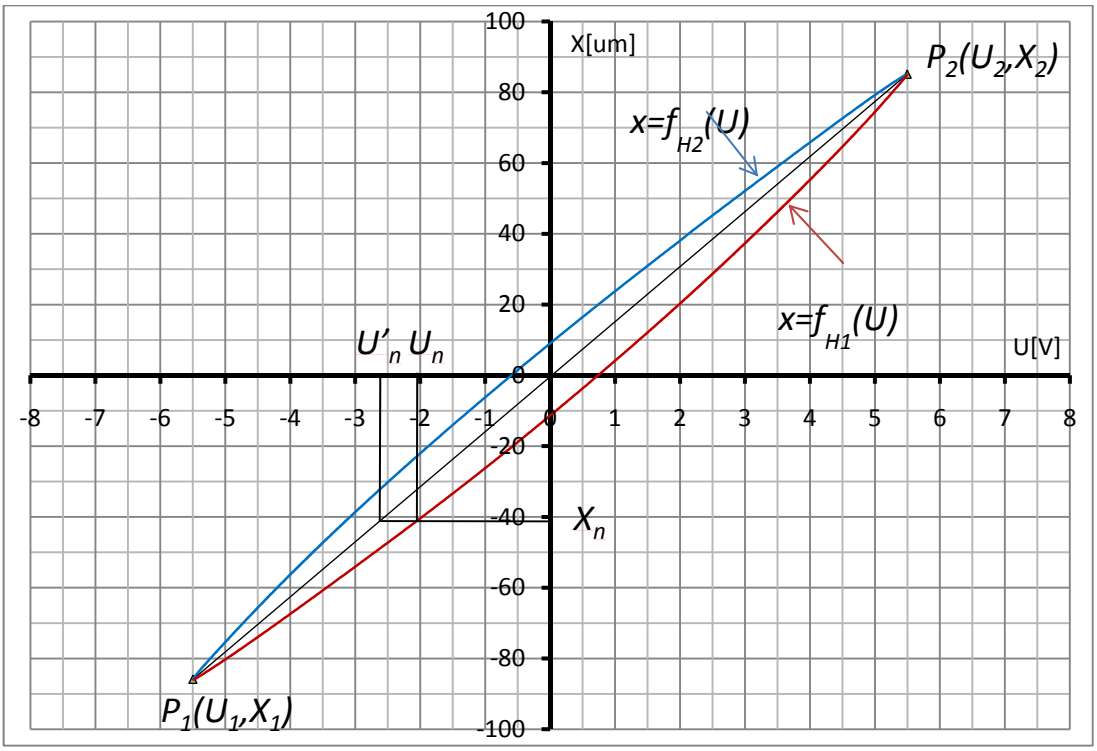

Figure 8: Outer hysteretic loop (refer to the text above for detailed explanation).

Following mathematical equations (1, 2, 3, 4) were used for U_A calculation:

$$U_A = U_n - U'_n \tag{1}$$

$$U_n = {f_{H1}}^{-1}(X_n) \ \ when \ \ U \ \nearrow \tag{2}$$

$$U_n = {f_{H2}}^{-1}(X_n) \ \ when \ \ U \ \searrow \tag{3}$$

$$U'_n = \frac{X_n - b}{a}, \ a = \frac{X_2 - X_1}{U_2 - U_1}, \ b = \frac{U_2 X_1 - U_1 X_2}{U_2 - U_1} \tag{4}$$

The results of calculation are presented graphically in Figure 9 (depicted as blue and red points). Data thus obtained were learning data for neural networks, NN_1 & NN_2. The neural network responses to the constraint U, ranging from U_1 to U_2, are depicted accordingly, by blue and red lines.

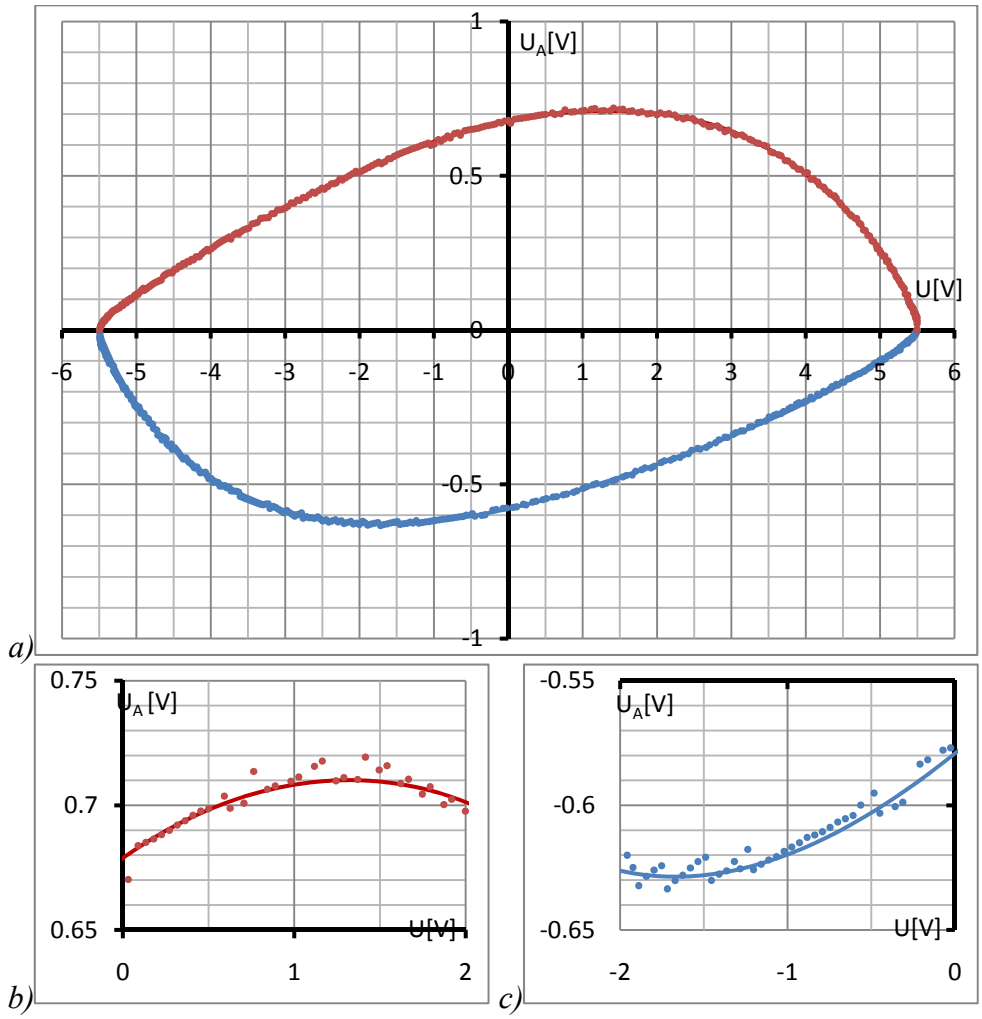

Figure 9: Graphs depicting U_P for the increasing (red dots) and decreasing (blue dots) constraining signal U and the neural network responses to the constraint (red line for increasing U, blue line for decreasing U):
a) entire graph, b) decreasing constraining signal (zoom-in),
c) increasing constraining signal (zoom-in).

The starting point of the compensating system activity was characterized by the constraining signal $U = 0[V]$ and the adjustment signal $U_A = 0[V]$, and defined as the zero turning point, $P_{T0}(U_{PZ0}, X_{PZ0})$. Each consecutive local point of the input signal extreme was denoted as the turning point $P_{Tn}(U_{Tn}, U_{ATn})$. Only the last turning point was saved by the system during the compensation progress. According to the input signal direction variation, direction factors a_n and b_n of the linear function crossing the turning point $P_{Tn}(U_{Tn}, U_{ATn})$ and the $P_{A2}(U_2, U_2)$, for the increasing signal, or $P_{A1}(U_1, U_1)$, for signal decrease, were determined (Figure 10). Appropriate scaled values calculated by the corresponding neural networks U_{NN} (NN_1 for the increasing

and NN_2 for the decreasing constraining signal U) were added to the linear function value U_L at point U calculated in equations (5, 6, 7).

$$U_P = U_1 \ when \ U \searrow \tag{5}$$

$$U_P = U_2 \ when \ U \nearrow \tag{6}$$

$$U_L = a_n U + b_n, \ a_n = \frac{U_{ATn} - U_P}{U_{Tn} - U_P}, \ b_n = \frac{U_P(U_{Tn} - U_{ATn})}{U_{Tn} - U_P} \tag{7}$$

The neural network response scaling factor was determined as the quotient of the current hysteretic arm length (distance between U_{Tn}, and U_1 or U_2, depending on the signal direction) and the outer hysteretic loop arm length (distance between U_2 and U_1).

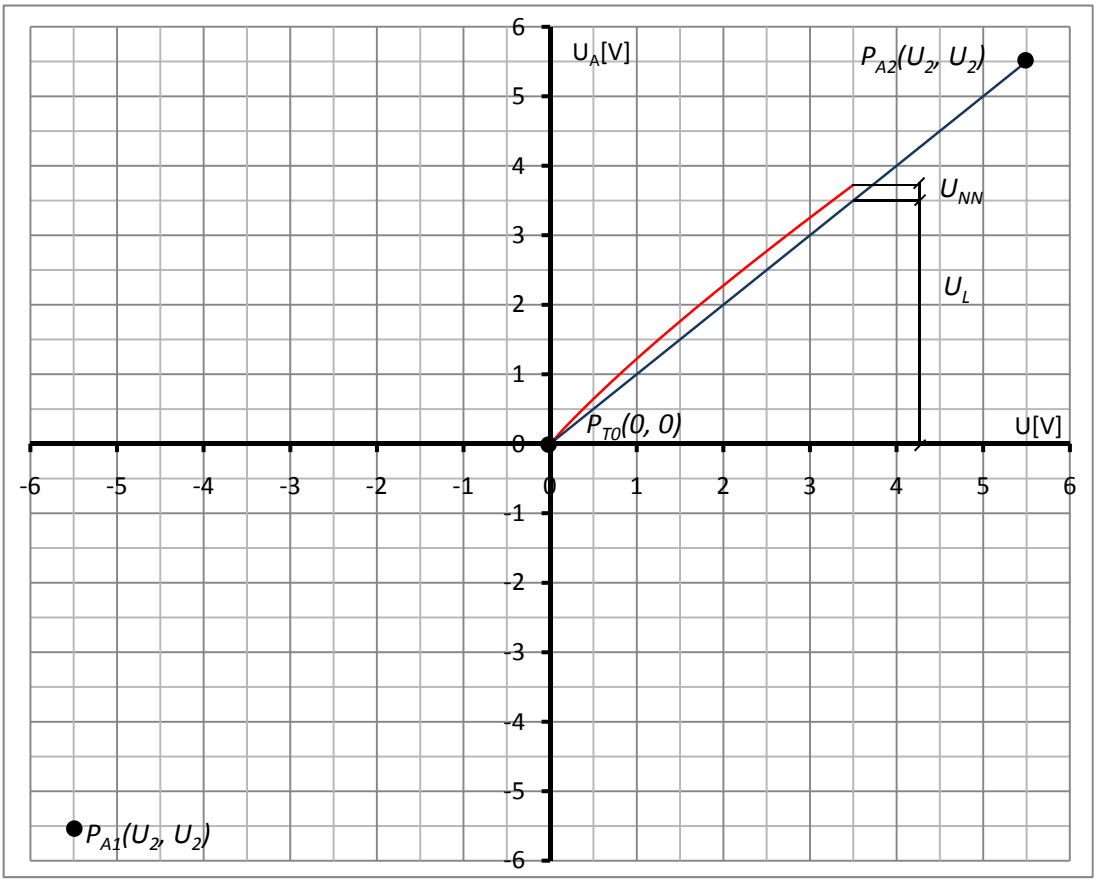

Figure 10: Starting point of compensating system activity
(linear function crossing P_{T0} and P_{A2}).

The constraint direction transition detected by the system automatically resulted in recording a new transition point $P_{Tn}(U_{Tn}, U_{ATn})$ (Figure 11). The point abscissa constituted the current value of the constraining signal U, while the point ordinate represented the previous iteration X value. Thus, new a_n and b_n parameters were allotted for the linear function connecting the turning point $P_{Tn}(U_{Tn}, U_{ATn})$ with $P_{A1}(U_1, U_1)$ for decreasing signal U or $P_{A2}(U_2, U_2)$ for increasing signal U.

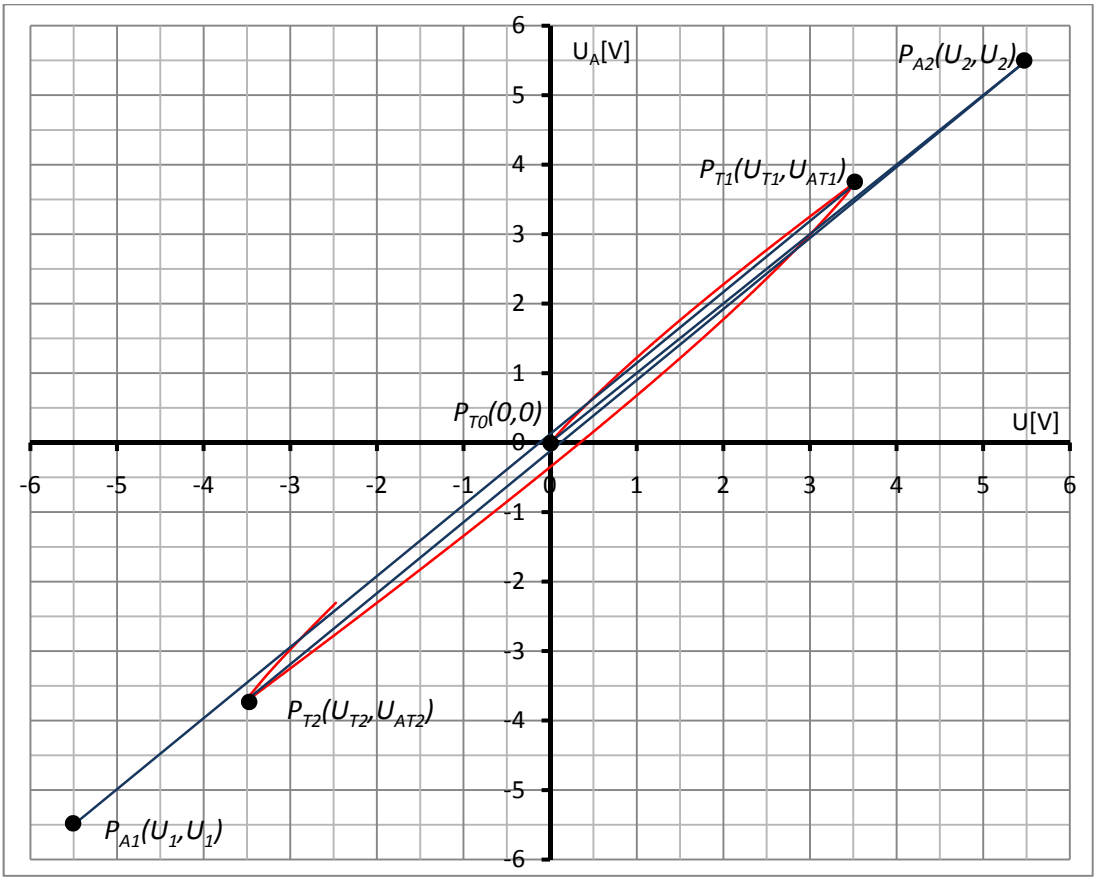

Figure 11: Local constraining signal extremes: P_{T0}, P_{T1}, & P_{T2}, and their connecting lines with P_{A1} and P_{A2}.

The control algorithm performing the aforementioned operations is illustrated in Figure 12.

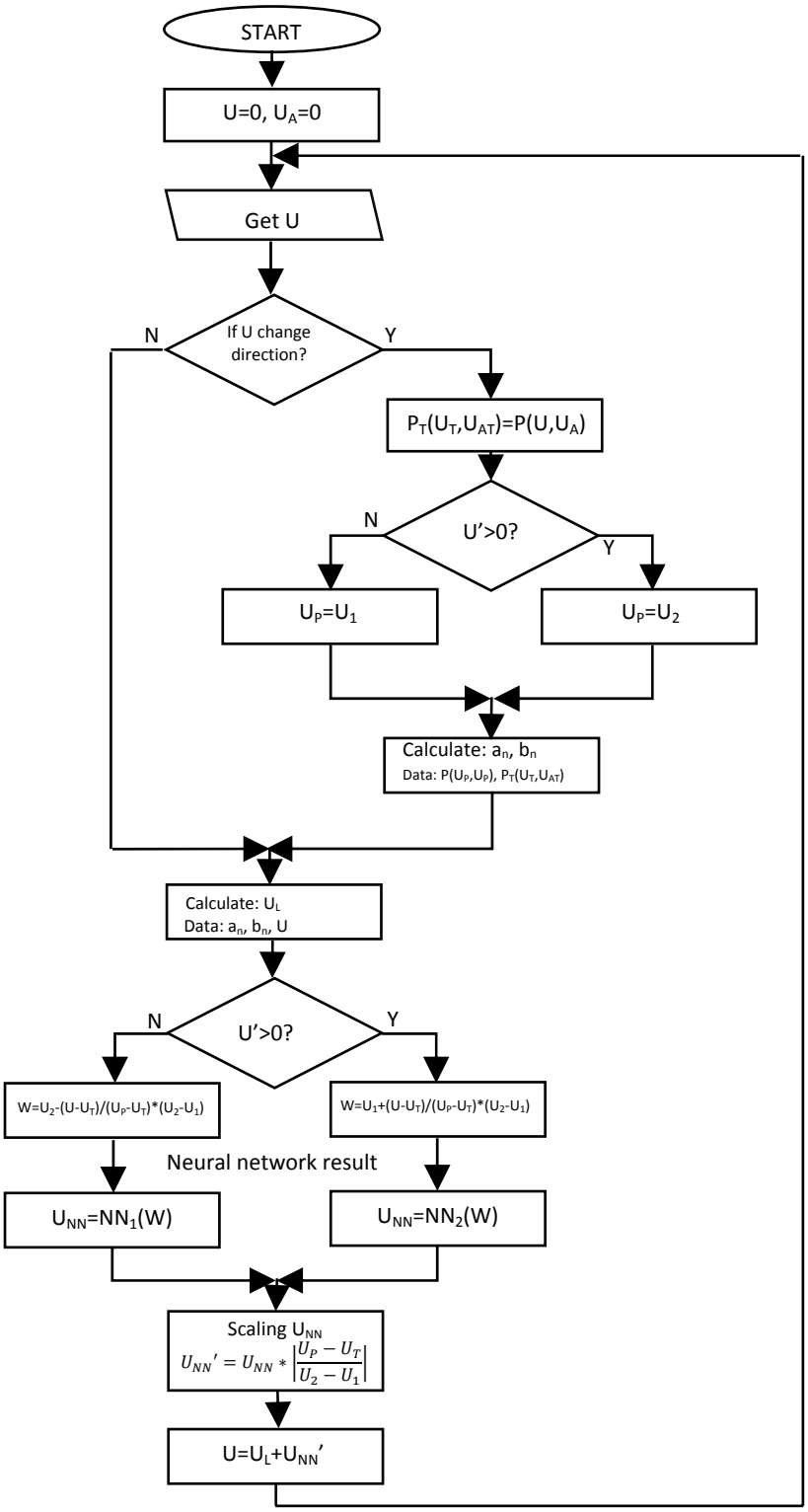

Figure 12: Hysteresis compensation control algorithm

5 Experimental results

Hysteresis linearization for the tested piezo bender actuators was investigated under the aforementioned data acquisition conditions. The obtained results are presented in Figures 13 and 14.

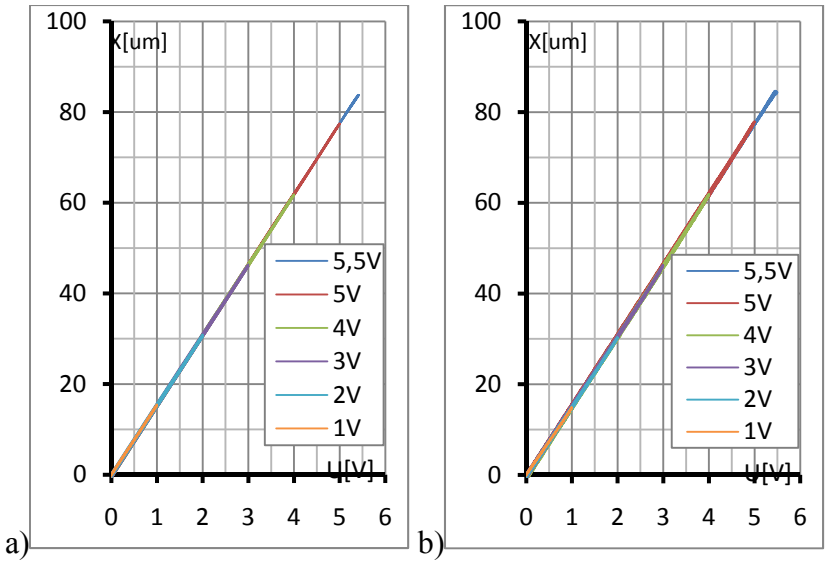

Figure 13: Hysteresis compensation investigation utilizing the piezo bender Pi Ceramic neural networks: a) simulation, b) experimental results.

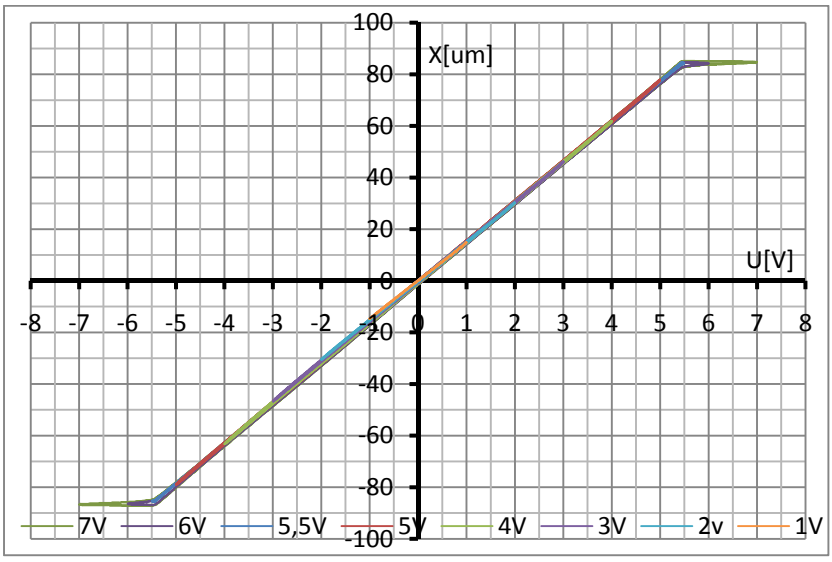

Figure 14: Piezo bender actuator investigation with hysteresis compensation for the constraint of 1 – 7 V.

6 Conclusions

The piezo bender actuator hysteresis compensation by means of the reverse profiling model was highly effective, resulting in hysteretic width reduction for all constraining signal amplitudes. As a result of the specific features of the introduced compensating system (no feedback loop) as well as the means of data acquisition, further applied in the linearization process, the proposed system operates properly only under quasi-static constraints. However, the restricted application range is not a limitation in the case of utilization of the piezo bender actuators as nozzle diaphragm drives in the electrohydraulic servo valve control stage. Compensation of the non-linearity of the entire drive (the piezo bender actuator as well as amplifier) constitutes an additional benefit. Furthermore, piezo bender actuators could be employed as compensator-coupled drives of optical measuring system lenses, electro-sonic converters, and many more devices.

References

[1] Noliac, www.noliac.com/Plate_benders-57.aspx
[2] Piceramic, www.piceramic.com/prdetail.php?sortnr=103000
[3] G. Bertotti, I. D. Mayergoyz, "The Science of Hysteresis, Chapter 4 Hysteresis in Piezoelectric and Ferroelectric Materials", ISBN: 978-0-12-480874-4, 337–465, 2006
[4] Noliac, www.noliac.com/Material_characteristics_-143.aspx
[5] Piceramic, www.piceramic.com/piezo_effect.php
[6] Piceramic, www.piceramic.com/piezo_tutorial5.php
[7] Noliac, www.noliac.com/Default.aspx?ID=739&NPMode=View&ProductID=27
[8] PI Ceramic, www.piceramic.com/prspecs.php?sortnr=103000
[9] D. Sędziak, M. Pelic, "The modeling of electrohydraulic servovalve with piezobender and electronic feedback" (in Polish), Archives of Mechanical Technology and Automation, 28, 79-88, 2008
[10] Noliac, www.noliac.com/Static_and_quasi-static_operation-6587.aspx
[11] Piceramic, www.piceramic.com/piezo_tutorial8.php
[12] H. Janocha, K. Kuhnen, "Real-time compensation of hysteresis and creep in piezoelectric actuators", Sensors and Actuators A: Physical,79(2), 83–89, 2000
[13] J.-J. Tzen, S.-L. Jeng, W.-H. Chieng, "Modeling of piezoelectric actuator for compensation and controller design", Precision Engineering, 27(1), 70–86, 2003
[14] C. Ru, L. Sun, "A new open-loop driving method of piezoelectric actuator for periodic reference inputs", Ultrasonics, 44 Supplement, e633–e637, 2006
[15] R. Changhai, S. Lining, "Hysteresis and creep compensation for piezoelectric actuator in open-loop operation", Sensors and Actuators A: Physical, 122 (1), 124–130, 2005

[16] T.-J. Yeh, R.-F. Hung, S.-W. Lu, “An integrated physical model that characterizes creep and hysteresis in piezoelectric actuators”, Simulation Modelling Practice and Theory, 16(1), 93–110, 2008

[17] C. Ru, L. Chen, B. Shao, W. Rong, L. Sun, “A hysteresis compensation method of piezoelectric actuator: Model, identification and control”, Control Engineering Practice, 17(9), 1107–1114, 2009

[18] L. Gaul, J. Becker, “Model-based piezoelectric hysteresis and creep compensation for highly-dynamic feed forward rest-to-rest motion control of piezoelectrically actuated flexible structures”, International Journal of Engineering Science, 47(11–12), 1193–1207, 2009

[19] J. Minase, T.-F. Lu, B. Cazzolato, S. Grainger, “A review, supported by experimental results, of voltage, charge and capacitor insertion method for driving piezoelectric actuators”, Precision Engineering, 34(4), 692–700, 2010

[20] P. Ge, M. Jouaneh, “Generalized preisach model for hysteresis nonlinearity of piezoceramic actuators”, Precision Engineering, 20(2), 99–111, 1997

[21] H. Hu, R. B. Mrad, “On the classical Preisach model for hysteresis in piezoceramic actuators:, Mechatronics, 13(2), 85–94, 2002

[22] L. Liu, K.-K. Tan, S.-L. Chen, S. Huang, T. -H. Lee, “SVD-based Preisach hysteresis identification and composite control of piezo actuators“, ISA Transactions, Available online, 2012

[23] D. Schonfeld, G. Friedman, “On the optimality of hysteresis operators in signal processing and communication systems”, Journal of the Franklin Institute, 342(7), 2005

[24] Q. Xu, P.-K. Wong, “Hysteresis modeling and compensation of a piezostage using least squares support vector machines”, Mechatronics, 21(7), 1239–1251, 2011

[25] O. G.-Bellmunt, F.-al Ikhouane, D. Montesinos-Miracle, “Control of a piezoelectric actuator considering hysteresis”, Journal of Sound and Vibration, 326(3–5), 383–399, 2009

[26] X. Zhao, Y. Tan, “Neural network based identification of Preisach-type hysteresis in piezoelectric actuator using hysteretic operator”, Sensors and Actuators A: Physical, 126(2), 306–311, 2006

[27] R. Dong, Y. Tan, H. Chen, Y. Xie, “A neural networks based model for rate-dependent hysteresis for piezoceramic actuators”, Sensors and Actuators A: Physical, 143(2), 370–376, 2008

[28] L. Deng, Y. Tan, “Diagonal recurrent neural network with modified backlash operators for modeling of rate-dependent hysteresis in piezoelectric actuators”, Sensors and Actuators A: Physical, 148(1), 259–270, 2008

[29] X. Zhang, Y. Tan, M. Su, “Modeling of hysteresis in piezoelectric actuators using neural networks”, Mechanical Systems and Signal Processing, 23(8), 2699–2711, 2009

[30] X. Zhang, Y. Tan, “A hybrid model for rate-dependent hysteresis in piezoelectric actuators”, Sensors and Actuators A: Physical, 157(1), 54–60, 2010

[31] X. Zhang, Y. Tan, M. Su, Y. Xie, “Neural networks based identification and compensation of rate-dependent hysteresis in piezoelectric actuators”, Physica B: Condensed Matter, 405(12), 2687–2693, 2010
[32] J.-D. Kim, S.-R. Nam, “An improvement of positioning accuracy by use of piezoelectric voltage in piezoelectric driven micro positioning system simulation”, Mechanism and Machine Theory, 30(6), 819–827, 1995
[33] J. Schäfer, H. Janocha, “Compensation of hysteresis in solid-state actuators”, Sensors and Actuators A: Physical, 49(1–2), 97–102, 1995
[34] U.-X. Tan, W. T. Latt, F. Widjaja, C. Y. Shee, C. N. Riviere, W. T. Ang, “Tracking control of hysteretic piezoelectric actuator using adaptive rate-dependent controller”, Sensors and Actuators A: Physical, 150(1), 116–123, 2009
[35] L. Deng, Y. Tan, “Modeling hysteresis in piezoelectric actuators using NARMAX models”, Sensors and Actuators A: Physical, 149(1), 106–112, 2009
[36] M.-J. Janga, C.-L. Chenb, J.-R. Leea, “Modeling and control of a piezoelectric actuator driven system with asymmetric hysteresis”, Journal of the Franklin Institute, 346(1), 17–32, 2009
[37] J. Park, W. Moon, “Hysteresis compensation of piezoelectric actuators: The modified Rayleigh model”, Ultrasonics, 50(3), 335–339, 2010
[38] G. Aguirre, T. Janssens, H. Van Brussel, F. Al-Bender, “Asymmetric-hysteresis compensation in piezoelectric actuators”, Mechanical Systems and Signal Processing, Available online, 2011
[39] L. Juhász, J. Maas, B. Borovac, “Parameter identification and hysteresis compensation of embedded piezoelectric stack actuators”, Mechatronics, 21(1), 329–338, 2011
[40] G. Y. Gu, L. M. Zhu, “Modeling of rate-dependent hysteresis in piezoelectric actuators using a family of ellipses”, Sensors and Actuators A: Physical, 165(2), 303–309, 2011
[41] A.-F. Boukari, J.-C. Carmona, G. Moraru, F. Malburet, A. Chaaba, M. Douimi, “Piezo-actuators modeling for smart applications”, Mechatronics, 21(1), 339–349, 2011